Correlation of tumor growth suppression and methionine aminopetidase-2 activity blockade using an orally active inhibitor

Jieyi Wang*, Lora A. Tucker, Jason Stavropoulos, Qian Zhang, Yi-Chun Wang, Gail Bukofzer, Amanda Niquette, Jonathan A. Meulbroek, David M. Barnes, Jianwei Shen, Jennifer Bouska, Cherrie Donawho, George S. Sheppard, and Randy L. Bell

Global Pharmaceutical Research and Development, Abbott Laboratories, 100 Abbott Park Road, Abbott Park, IL 60064

Edited by Brian W. Matthews, University of Oregon, Eugene, OR, and approved December 20, 2007 (received for review September 17, 2007)

This laboratory and others have shown that agents that inhibit the *in vitro* catalytic activity of methionine aminopeptidase-2 (MetAP2) are effective in blocking angiogenesis and tumor growth in preclinical models. However, these prototype MetAP2 inhibitors are clearly not optimized for therapeutic use in the clinic. We have discovered an orally active class of MetAP2 inhibitors, the anthranilic acid sulfonamides exemplified by A-800141, which is highly specific for MetAP2. This orally bioavailable inhibitor exhibits an antiangiogenesis effect and a broad anticancer activity in a variety of tumor xenografts including B cell lymphoma, neuroblastoma, and prostate and colon carcinomas, either as a single agent or in combination with cytotoxic agents. We also have developed a biomarker assay to evaluate *in vivo* MetAP2 inhibition in circulating mononuclear cells and in tumors. This biomarker assay is based on the *N*-terminal methionine status of the MetAP2-specific substrate GAPDH in these cells. In cell cultures *in vitro*, the sulfonamide MetAP2 inhibitor A-800141 caused the formation of GAPDH variants with an unprocessed N-terminal methionine. A-800141 blocked tumor growth and MetAP2 activity in a similar dose–response in mouse models, demonstrating the antitumor effects seen for A-800141 are causally connected to MetAP2 inhibition *in vivo*. The sulfonamide MetAP2 inhibitor and GAPDH biomarker in circulating leukocytes may be used for the development of a cancer treatment.

angiogenesis | biomarker | cancer therapy | GAPDH | MetAP2

Eukaryotic proteins are synthesized on the ribosome with an N-terminal methionine. In the majority of cellular proteins, the methionine is removed cotranslationally (1), and this removal of the initiator methionine is required for proper function of these proteins, i.e., activity, localization, and stability. N-terminal methionine processing is accomplished by the action of two intracellular metalloproteases: methionine aminopeptidase 1 and 2 (MetAP1 and MetAP2) (2, 3). Recently, evidence for an additional mammalian enzyme, MAP1D (or MetAP3), has been shown (4). Although very little is known about the new protein, it appears to be localized in the mitochondria and to resemble MetAP1 in several respects, including high amino acid homology and similar inhibitor sensitivity. The differential physiological responsibilities of MetAP1 and MetAP2 are not clearly understood. These two enzymes are both associated with the ribosome and could compensate for each other (5). MetAP1 and MetAP2 double-null yeast strains are nonviable, but the MetAP1- or MetAP2-null strain is viable, albeit with a slower growth rate (5, 6). In addition, overall protein *N*-myristoylation is unaffected in endothelial cells treated with the selective MetAP2 inhibitor TNP-470, suggesting that MetAP1 activity can generally compensate when MetAP2 is inactive (6). MetAP1 and MetAP2 are dissimilar in a number of key respects. These include substrate specificity and expression control. For example, MetAP2 is able to process a limited set of proteins untouched by MetAP1 (6). In addition, induction of MetAP2 expression is associated with cell proliferation, whereas MetAP1 is constitutively expressed (7, 8). More recently, MetAP1 has been shown to play a role in the G_2/M phase of cell cycle (9), whereas MetAP2 inhibition leads to G_1 arrest (10–12).

Many of the details of the function of MetAP2 and its role in cell physiology are still unknown. In addition to its methionine aminopeptidase activity, MetAP2 has a second function: the stabilization of eIF-2α phosphorylation status (8). That MetAP2 is a bifunctional protein complicates the study of its function with deletion or siRNA techniques, because the eIF-2α has an important role in controlling protein synthesis and cell growth (8). Recently, it has been reported that MetAP2 knockout mouse embryos fail to undergo gastrulation, and targeted knockout of MetAP2 in the hemangioblast lineage caused abnormal vascular development and a lethal phenotype at the midsomite stage (13). These results clearly demonstrate an essential role of MetAP2 in embryonic development and vasculogenesis. Antisense and siRNA also have been used to examine the role of MetAP2. Knockdown of MetAP2 results in cell growth inhibition and apoptosis in endothelial and tumor cells (13–15). The antiproliferative phenotype of MetAP2 knockdown can be recapitulated by the inhibition of the enzymatic activity of MetAP2. The natural product fumagillin and its analog TNP-470 (16) selectively block MetAP2 activity and inhibit endothelial cell proliferation through a p53-dependent induction of $p21^{WAF1/CIP1}$ (11, 12). It is well established that TNP-470 has strong antiangiogenesis effects and inhibits tumor growth in a variety of experimental models (16, 17). The rationally designed reversible MetAP2 inhibitor, A-357300, shows a similar antiproliferation profile to that of fumagillin and suppresses tumor growth in mouse models (10). However, an *in vivo* correlation of MetAP2 inhibition with tumor suppression remains to be established.

Correlating target inhibition (biomarker) and efficacy has become an important endeavor in the development of targeted cancer therapies. An assay for active cellular MetAP2 enzyme has been reported (6, 18), but it can be used only for irreversible MetAP2 inhibitors. MetAP2 removes the N-terminal methionine in selected protein substrates (6), and these specific cellular proteins provide potential biomarkers for MetAP2 inhibition. In this report, we demonstrate a correlation of MetAP2 inhibition and tumor response *in vivo* using a biomarker system based on the MetAP2 specific substrate GAPDH in both tumors and circulating mononuclear cells, with an orally active series of MetAP2 inhibitors.

Author contributions: J.W., C.D., and R.L.B. designed research; J.W., L.A.T., J. Stavropoulos, Q.Z., Y.-C.W., G.B., A.N., J.A.M., J. Shen, J.B., and C.D. performed research; D.M.B. and G.S.S. contributed new reagents/analytic tools; J.W., C.D., G.S.S., and R.L.B. analyzed data; and J.W., L.A.T., and R.L.B. wrote the paper.

The authors declare no conflict of interest.

This article is a PNAS Direct Submission.

*To whom correspondence should be addressed. E-mail: jieyi.wang@abbott.com.

This article contains supporting information online at www.pnas.org/cgi/content/full/0708766105/DC1.

© 2008 by The National Academy of Sciences of the USA

Fig. 1. Comparison of MetAP2 binding of A-800141 and A-357300 by crystallography. *Upper* shows the chemical structure of the sulfonamide inhibitor A-800141 and the bestatin inhibitor A-357300. *Lower* shows an overlay of crystal structure of MetAP2 active site with A-800141 (in magenta) and A-357300 (in green). The two manganese ions in the MetAP2 active site are shown in blue. Reference residues include His-231, the residue alkylated by fumagilin and its semisynthetic derivatives (23), and Tyr-444, which terminates the 60-aa insert that forms a portion of the hydrophobic pocket of the MetAP2 active site.

Results

The Aryl Sulfonamide MetAP2 Inhibitor A-800141 Possesses Strong Antitumor Activity. We have shown that a rationally designed bestatin-type inhibitor of MetAP2, A-357300, induces cytostasis by cell cycle arrest at the G_1 phase in endothelial cells and certain tumor cells, and that this MetAP2 inhibitor blocks angiogenesis and shows potent antitumor efficacy in carcinoma, sarcoma, and neuroblastoma murine models (10, 19). More recently, we have reported that the most potent and selective MetAP2 inhibitors we discovered thus far are compounds of an anthranilic acid aryl sulfonamide series, originally identified by mass spectrometry-based affinity selection screening (20–22). Initial screening hits were modified with the aid of multiple crystal structures compared obtained with A-357300 (10). X-ray cocrystal structures indicate that the aryl sulfonamide class of MetAP2 inhibitors, exemplified by A-800141 (Fig. 1), interacts at the MetAP2 active site with the anthranilic acid carboxylate coordinating one of the two manganese ions. In contrast, A-357300 cocrystalizes with the 2-hydroxy-3-amino amide functional array interacting with both manganese centers with an oxygen bridging between them. The tetrahydronaphthalene rings of A-800141 fully occupy the hydrophobic region of the active site adjacent to the 60-aa insert ending in Tyr-444, whereas A-357300 partially fills this space (Fig. 1). The aryl sulfonamide portion of A-800141 occupies a hydrophobic cleft on the enzyme surface adjacent to the active site, which is solvent-exposed on one edge, allowing the introduction of the (*Z*)-3-diethylamino-prop-1-enyl group, which improves the solubility and modulates the albumin-binding properties of A-800141 (21).

We tested A-800141 against a panel of aminopeptidases. A-800141 showed potent activity against MetAP2 with an IC_{50} of 12 nM (Table 1) with a high selectivity. The only other aminopeptidase examined to date showing inhibition by this sulfonamide inhibitor at high concentrations was MetAP1 (Table 1). Although

Table 1. Comparison of the *in vitro* activity of MetAP2 inhibitors A-800141, TNP-470, and A-357300

Compound	TNP-470	A-800141	A-357300
Enzyme activity IC_{50}, μM			
MetAP2	0.008	0.012	0.12
MetAP1	>10	36	57
Aeromonas aminopeptidase	>10	>100	11
LAP	>10	>100	9
LTA4 hydrolase	>10	>100	>100
Cell proliferation IC_{50}, μM			
HMVEC	0.001	0.010	0.1
HT1080	0.003	0.026	0.2
HCT116	0.002	0.018	0.3
A549	0.004	0.025	0.2
NCI-H460	0.003	0.011	0.1
B16F10	0.002	0.011	0.3

both MetAP2 and MetAP1 enzymes share a common "pita fold" structure and have two metal ions in the active site, MetAP2 contains a 60-aa insert that results in a larger active site (2, 10, 23, 24) (Fig. 1). As a result, A-800141 showed a 3,000-fold selectivity between MetAP1 and MetAP2. In addition, kinetic analysis indicated that A-800141 is reversible against MetAP2 [supporting information (SI) Fig. 5]. A-800141 also showed a greater selectivity against other aminopeptidases than the bestatin inhibitor A-357300. In addition, A-800141 was found to be inactive against elastase, cathepsin B, chymotrypsin types 2 and 7, kallikrein, and urokinase at up to 100 μM concentrations. A-800141 at 10 μM did not show any significant receptor binding, as determined in a CEREP panel of >80 receptors. Thus, A-800141 is a highly selective inhibitor for MetAP2.

The aryl sulfonamide A-800141 is also a potent inhibitor of cell proliferation (Table 1). The antiproliferative activity of A-800141 was not limited to endothelial cells, as originally proposed for fumagillin and TNP-470 (16), but extended to many tumor cell lines as well, which is described in detail elsewhere (25). The antiproliferative activity of the sulfonamide series of inhibitors has been shown to correlate tightly with their cellular activity inhibiting MetAP2 enzyme function (21). The effect of MetAP2 inhibitors was cytostatic; treated cells were arrested in the G_1 phase of cell cycle without apoptosis. As shown in SI Fig. 6, A-800141, like TNP-470, caused a cell cycle arrest in the G_1 phase in HUVEC. The potency of A-800141 in inducing G_1 arrest was similar to that of inhibition of proliferation. A-800141 started to show an effect at 10 nM but induced a significant increase of cells in G_1 (54% vs. 39%) at 100 nM after 24 h of treatment. Higher concentrations of A-800141 (100 μM) and longer time (3 days) incubation resulted in a similar G_1 arrest cell cycle profile (SI Fig. 6), suggesting a highly selective nature of this compound in cells. We also analyzed p53, p21, Rb, and cyclin proteins in HUVEC treated with these MetAP2 inhibitors to ensure a consistent effect on these cell cycle markers among these distinct classes of compounds. Both TNP-470 and A-800141 resulted in an elevation of p21 in HUVEC and a modest increase of p53 (SI Fig. 7). Reduction of phosphorylated Rb and total level of cyclin A were also a consistent consequence of treatment with TNP-470, A-800141 (SI Fig. 7), and A-357300 (10). Therefore, we have discovered a series of MetAP2 inhibitors that are highly selective and possess potent antiproliferative activity against endothelial cells and tumor cells with IC_{50} values <100 nM.

MetAP2 inhibitor A-800141 has a broad antitumor activity *in vivo*. The compound was found to be effective in a flank tumor growth model using the human neuroblastoma cell line CHP-134. This line has amplified *N*-myc, which is characteristic of the most aggressive neuroblastomas seen in cancer patients (19). The CHP-134 tumor was staged at 200 mm^3 in female SCID mice and A-800141 administered at 150 mg/kg per day and 75 mg/kg per day

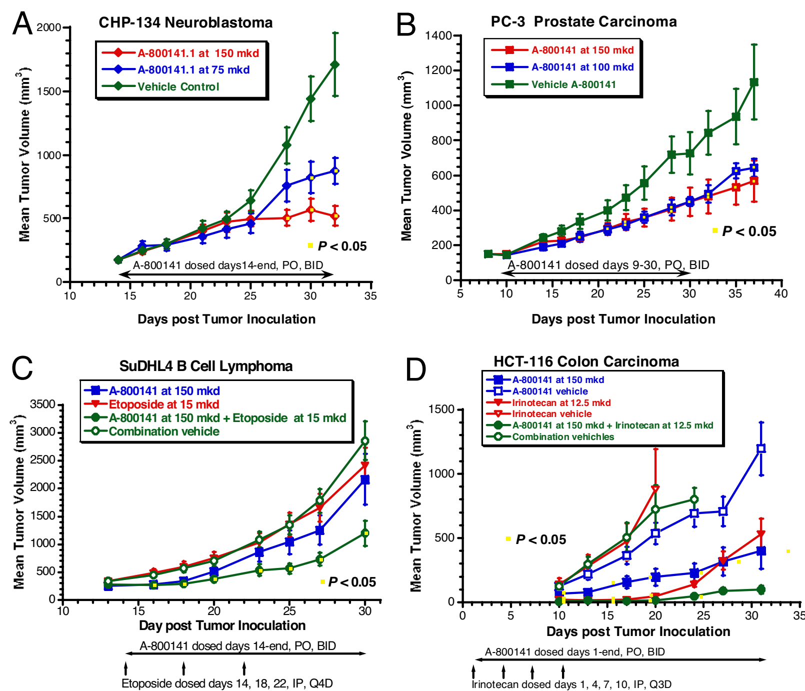

Fig. 2. A-800141 shows a broad range of antitumor activity in mouse xenograft models. (*A*) CHP-134 human neuroblastoma in SCID female mice. (*B*) PC-3 human prostate carcinoma in SCID male mice. (*C*) SuDHL4 human B cell lymphoma in male SCID beige mice. (*D*) HCT-116 human colon carcinoma in SCID female mice. Mice were randomized into treatment groups as shown ($n = 10$). Dosages were shown as total mg/kg per day (mkd) that were given p.o. twice daily every day during therapy period as shown (A-800141) or by i.p. Q4D (Etoposide) or i.p. Q3D (Irinotecan). The yellow squares indicate $P < 0.05$ for comparing the tumor sizes between the treatment and control groups.

by twice-daily oral gavages. As shown in Fig. 2*A*, both doses gave significant inhibition of tumor growth. A-800141 dosed at 150 mg/kg/day showed 70% tumor growth inhibition and was well tolerated without overt toxicity. The efficacy of this MetAP2 inhibitor for treating neuroblastoma in mouse models supports the contention that MetAP2 inhibitors may be useful for the treatment of this disease in the clinic (19). PC-3 human prostate carcinoma was another xenograft sensitive to treatment with A-800141. PC-3 cells were inoculated in the flank of SCID male mice. Treatment was initiated when the tumors reached 150 mm^3. As shown in Fig. 2*B*, A-800141 dosed at both 150 and 100 mg/kg per day by twice-daily oral gavages resulted in significant tumor growth delay.

MetAP2 inhibition causes growth arrest but not cell death to tumor cells while having perhaps a broader antitumor effect because of inhibition of angiogenesis. Like A-357300 (10), A-800141 significantly blocked growth factor induced neovessel formation in mouse cornea angiogenesis models (see below). Given the dual actions on tumor cells and endothelial cells by MetAP2 inhibitors, we were interested in combining this mechanism of cancer therapy with cytotoxic chemotherapeutics. Several agents were examined in combination with A-800141 to probe the potential for additivity or perhaps synergy in mouse tumor models. Agents studied included etoposide, a topoisomerase II inhibitor, irinotecan, a DNA topoisomerase I inhibitor, ABT-737 developed at Abbott Laboratories as a BCL2 directed antiapoptotic agent (26), and 5-fluoracil and cyclophosphamide. A-800141 and etoposide were examined in a human B cell lymphoma xenograft model designated SuDHL4 in female SCID-beige mice (Fig. 2*C*). Neither agent alone was effective in slowing tumor growth in this model, but the combination treatment showed significant tumor inhibition. No issues of toxicity were seen throughout the course of the trial in any groups. In another human B cell lymphoma xenograft (DOHH-2), combination of a sulfonamide MetAP2 inhibitor with the BCL-2 inhibitor ABT-737 (26) resulted in a significant additive activity of 76% tumor growth inhibition (data not shown). These data support that MetAP2 inhibitors may be used for the treatment of B cell lymphoma, where overexpression of MetAP2 has been documented (27). Irinotecan was tested in combination with A-800141 against HCT-116 human colon carcinoma xenograft in a flank tumor model performed in female SCID mice. As shown in Fig. 2*D*, both irinotecan and A-800141 were effective as single therapy in slowing the tumor growth in this early intervention trial. Irinotecan alone produced nearly complete tumor inhibition until day 20, but the tumor grew back subsequently. The tumor rebound was significantly suppressed when A-800141 was given in combination with irinotecan (Fig. 2*D*).

Taken together, the above data with this MetAP2 inhibitor and the literature on anticancer activities of other MetAP2 agents clearly demonstrate that MetAP2 inhibitors possess a strong antitumor activity. However, the question whether the antitumor efficacy is caused by MetAP2 inhibition by these agents has not been resolved. To address this question, we sought to develop a biomarker for MetAP2 inhibition *in vivo* and use it to correlate MetAP2 activity and tumor growth inhibition by various chemical classes of inhibitors.

GAPDH Is a Specific Substrate of MetAP2 and Provides a Biomarker for MetAP2 Inhibition *in Vivo*. GAPDH in bovine aortic endothelial cells (BAECs) was reported to be a MetAP2-specific substrate by Liu and coworkers (6). To confirm that GAPDH in human and murine cells is a MetAP2-specific substrate, we isolated GAPDH from human HT1080 fibrosarcoma cells and mouse bEND3 endothelial cells treated with 100 nM fumagillin, a highly specific MetAP2 inhibitor, and determined the N-terminal sequence of GAPDH in these preparations. The sequencing data showed that GAPDH from HT1080 cells treated with fumagillin had an unprocessed N-terminal methionine (N-terminal sequence MGKVK, 80%; GKVKV, 20%), whereas GAPDH from untreated cells lacked an N-terminal methionine (N-terminal sequence GKVKV, 100%). In the mouse bEND3 cells, we found that the GAPDH variant with unprocessed N-terminal methionine (MVKVG) was present only in fumagillin-treated cells and not in untreated controls. These data show that cellular GAPDH normally does not retain the N-terminal methione residue, and that MetAP2 is responsible for this processing.

GAPDH is a ubiquitously expressed high-abundance protein, and we reasoned it might serve as cellular marker for MetAP2 inhibition. We therefore initiated efforts to establish an assay to differentiate GAPDH variants with unprocessed N-terminal methionine from mature processed GAPDH. Based on the 2D gel

B	Proliferation EC_{50} (nM)	GAPDH EC_{50} (nM)
Fumagillin	5	4
A-357300	400	500
A-800141	20	20

Fig. 3. GAPDH is a biomarker for cellular MetAP2 inhibition *in vitro* and *in vivo*. (*A*) Mouse bEND3 cells were treated with fumagillin or A-357300 in dose ranges as shown for 48 h. Cellular GAPDH was analyzed by IEF/Western blot (*Left*). The bottom band of all samples was quantified by densitometry analysis and shown as percentage of total GAPDH (*Right*). (*B*) Comparison of EC_{50}s of proliferation inhibition and GAPDH variant induction by fumagillin, A-357300 and A-800141. (*C*) Analysis GAPDH in circulating WBCs from mice treated with TNP-470 or A-357300. Each lane represents the sample of one mouse. TNP-470 was dosed at 30 mg/kg by one s.c. injection each on days 1 and 3, and the leukocytes were harvested on day 4. A-357300 was administered at 100 mg/kg per day by s.c. injections twice daily for the duration as shown.

mobility shift of GAPDH from cells treated with TNP-470 (6), we speculated that 1D isoelectric-focusing electrophoresis (IEF) might separate the GAPDH variants with and without N-terminal methionine, and that IEF followed by immunoblot might provide an assay for GAPDH variants as a marker for cellular MetAP2 inhibition. With extensive experimentation, electrophoresis with a specific IEF gel of pI 7–9 followed by immunoblot was established to measure GAPDH variants in total cell lysates (SI Fig. 8*A*). Human HT1080 fibrosarcoma cells treated with the two chemical classes of MetAP2 inhibitors, fumagillin and A-357300 (10), had a new band with lower pI, appearing 7 h after incubation with these inhibitors (SI Fig. 8*A*). Mouse bEND3 cells treated with MetAP2 inhibitors showed two new bands of lower pI beginning at 7 h after drug exposure (SI Fig. 8*A*). The new band in human cells was the GAPDH variant with an unprocessed methionine as confirmed by LC-MS analysis (data not shown), and the two new bands in mouse cells were consistent with GAPDH variants with an unprocessed methionine and an unprocessed acetylated methionine, respectively (SI Fig. 8).

To determine whether MetAP2 inhibitors induce the GAPDH variants at concentrations effective for inhibition of proliferation *in vitro*, we studied the effect of fumagillin and A-357300 in bEND3 cells in a dose–response fashion (Fig. 3*A*). We chose bEND3 cells, because we wanted to use the technique in mouse models of angiogenesis and tumor growth. In addition, the GAPDH variant with an N-terminal acetylated methionine in mouse cells was better separated on the IEF gel, so it could be more clearly quantified by densitometry (Fig. 3*A*). MetAP2 inhibitors induced GAPDH variants in bEND3 cells in a dose-dependent fashion similar to that observed for their antiproliferative activity (proliferation IC_{50}s of 5 and 400 nM for fumagillin and A-357300, respectively) (Fig. 3*B*). Similar dose–response data were obtained also in HT1080 cells (data not shown). These data demonstrate there is a correlation between the GAPDH processing and proliferation inhibition induced by MetAP2 inhibitors, indicating that these compounds act on mechanism, and that GAPDH *N*-terminal status may be a biomarker for cellular MetAP2 inhibition *in vitro*.

To determine whether GAPDH could be used as a biomarker to follow MetAP2 inhibition *in vivo*, we sought to analyze GAPDH in circulating white blood cells (WBC) from mice treated with MetAP2 inhibitors. First, WBC samples from immunocompetent C57Bl6 mice treated for 4 days with TNP-470 at 30 mg/kg by two s.c. injections on days 1 and 3, respectively, were assessed for GAPDH variants. GAPDH variants were detected in the TNP-470-treated mice (Fig. 3*C*). Next, we tested the time course of formation of GAPDH variants using the reversible inhibitor A-357300. C57Bl6 mice were dosed for 1–4 days with A-357300 at a dose of 100 mg/kg per day by s.c. injections twice daily. As shown in Fig. 3*C*, GAPDH variants were seen 3–4 days after initial dosing. A-357300 at a dose of 100 mg/kg per day given by s.c. injections twice daily was shown to be efficacious in suppressing tumor growth in several mouse models (10, 19). Together, these data suggest that GAPDH is a marker for MetAP2 inhibitor activity *in vivo*.

GAPDH Biomarker Correlates with Tumor Inhibition by A-800141 *in Vivo*. First, we tested A-800141 *in vitro* to see whether it could induce GAPDH variants in bEND3 cells in a manner similar to what we saw with A-357300 or fumagillin (Fig. 3). As shown in Fig. 4, GAPDH with unprocessed N-terminal methionine variants were detected in cells treated with A-800141 in a dose-dependent manner, with a 20 nM EC_{50}, which is identical to that for proliferation inhibition (20 nM). To estimate the potency of this compound in the physiological environment, we also tested A-800141 in bEND3 cells grown in the presence of 40 mg/ml human serum albumin. Protein binding affected the potency of this compound by 5- to 10-fold (Fig. 4). The EC_{50} was estimated to be 100 nM, similar to its antiproliferation potency measured in the presence of albumin. At concentrations ≥ 1 μM, A-800141 was able to cause nearly complete inhibition of cellular MetAP2 activity in the presence of physiological concentrations of human serum albumin. Next, we used A-800141 to examine whether the induction of GAPDH variants correlated with the *in vivo* antiangiogenic and antitumor activity of this agent. In the cornea angiogenesis model performed in CF1 outbred mice, VEGF-induced neovessel growth was significantly inhibited by A-800141 in a dose–response manner (Fig. 4*B*). In the same study, GAPDH in circulating WBC at the end of study was analyzed. As shown in Fig. 4*B*, the appearance of unprocessed GAPDH in these dosing groups was parallel to angiogenesis inhibition.

In the syngeneic, B16F10 melanoma, s.c. tumor model, A-800141 was effective in inhibiting tumor growth in this model when dosed orally. In three separate studies, doses of 150–200 mg/kg per day given by twice-daily oral gavage produced nearly complete inhibition of tumor growth. Dose–response data from one of the studies are shown in Fig. 4*C*. A-800141 dosed at 200 mg/kg per day by twice-daily oral gavages blocked GAPDH processing significantly, as indicated by the density (40% of total) of the lowest GAPDH band and disappearance of mature GAPDH in both WBCs and tumor tissues (Fig. 4*D*). As described above, this dose also produced 85% tumor growth inhibition. The degree of tumor growth inhibition tracks with the extent of methionine retention in GAPDH. These data further support that the N-terminal status of GAPDH in circulating mononuclear cells can be used as a biomarker to monitor MetAP2 inhibition in preclinical and potentially in clinical studies.

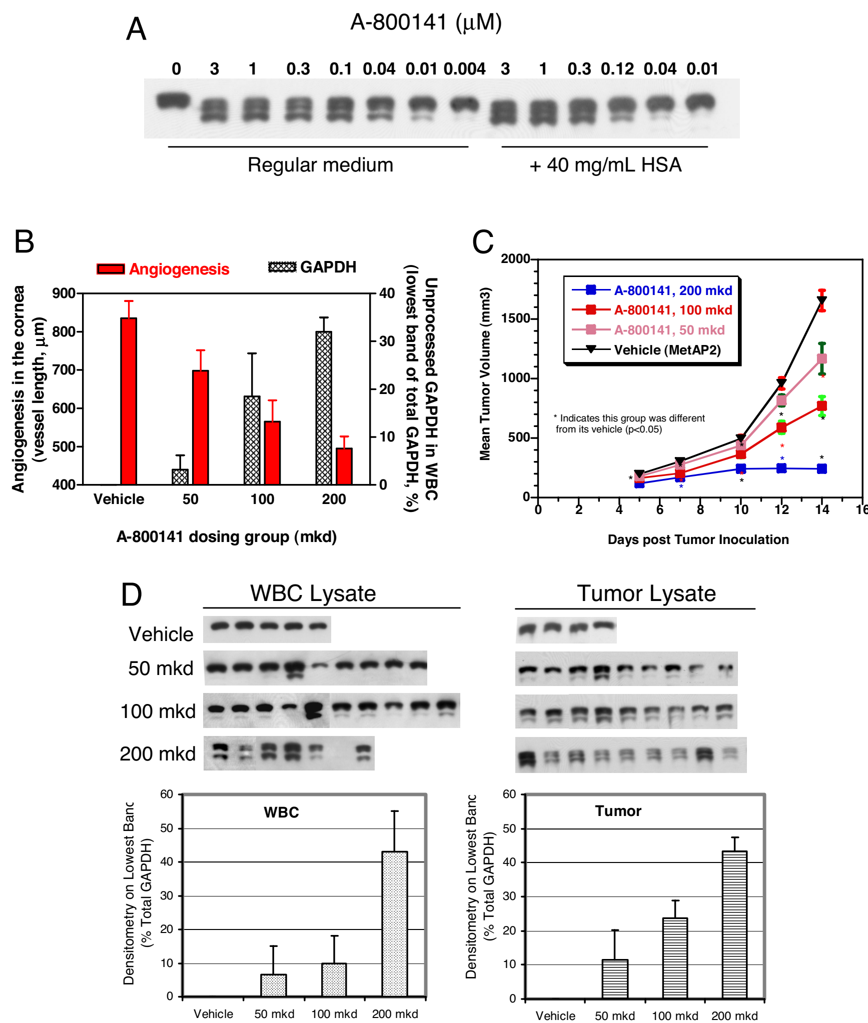

Fig. 4. A-800141 inhibits GAPDH processing and tumor growth in a similar dose–response. (*A*) IEF/Western blot analysis of GAPDH in mouse bEND3 cells. bEND3 cells were treated for 48 h with A-800141 in dose ranges as shown under regular growth medium (DMEM plus 10% FBS) or medium plus 40 mg/ml human serum albumin (HSA). (*B*) Inhibition of mouse cornea angiogenesis and GAPDH processing in CF1 female mice circulating WBCs. The effect on maximal neovessel length induced by VEGF was measured as described (10). Circulating WBCs in these mice at the end of study were isolated and subjected to analysis for GAPDH variants. (*C*) Inhibition of B16F10 melanoma tumor growth *in vivo*. B16F10 murine melanoma cells were inoculated in the flank of C57BL6 mice on day 0. Treatment started on day 1 and continued through day 14. Dosages were shown as total mg/kg per day (mkd) that were given p.o. twice daily every day during the therapy period as shown. The stars indicate $P < 0.05$ for comparing the tumor sizes between the treatment and control groups. (*D*) IEF/Western blot analysis of GAPDH in WBCs and tumor lysates. Samples were taken from mice in the B16F10 tumor trial shown in *C*. Each lane represents the sample from one mouse. The densitometry data are for each dosing groups.

Discussion

We have shown that reversible inhibition of MetAP2 can lead to suppression of tumor growth in mouse tumor models using the bestatin-type inhibitor A-357300 (10). Although this agent is quite effective in mouse models, it does not have the appropriate pharmaceutical properties to be a clinical candidate. In addition, data shown here indicate that it has other protease inhibitory activities that make it less specific than desired. Accordingly, we turned to a new class of MetAP2 inhibitors, the aryl sulfonamides, to explore the potential of those agents. The aryl sulfonamides bind to the enzyme active site in a different manner compared with A-357300 or TNP-470, as assessed by analysis of multiple crystal structures (10). The aryl sulfonamide molecule fully occupies the hydrophobic pocket in the MetAP2 active site with the tertrahydronaphthalene group, and it interacts with only one manganese ion in the active site (22). Multiple rounds of synthesis, enzyme testing, and crystal structures led eventually to potent, selective, reversible MetAP2 inhibitors exemplified here by A-800141. This MetAP2 inhibitor has 3,000-fold selectivity over MetAP1 and possesses nanomolar potency against the enzyme and in cell proliferation assays. Although cytostatic in their action, the potent aryl sulfonamides clearly are very effective antiproliferative agents.

The MetAP2 inhibitor A-800141 had significant single-agent activity in inhibiting tumor growth in several mouse tumor models. However, this activity did not extend to regression of tumors in our hands. This lack of tumor-killing activity can be traced to the fact that these agents are not cytotoxic *in vitro*, causing growth arrest but not apoptosis. This observation with the aryl sulfonamide class of inhibitors is consistent with data for the bestatin A-357300 and TNP-470. The tumor growth studies described here for the aryl sulfonamides provide additional support for the antitumor effects of MetAP2 inhibition. The cytostatic nature of MetAP2 inhibition and the potential of antiangiogenic effect motivated us to perform pilot experiments using combinations of MetAP2 inhibitors and several other agents. As shown above, the effects on tumor growth by the aryl sulfonamides in combination with irintotecan, etoposide, and a BCL-2 inhibitor clearly indicate the potential for combination dosing of several types of anticancer agents with MetAP2 inhibitors.

The correlation of inhibition of proliferation with broad methionine processing is supported by previous studies (10, 21). We have been able to expand this observation and provide more specific molecular characterization. Following up on the observation by Liu and colleagues (6), we examined GAPDH as a specific substrate of MetAP2. We developed a specific assay that allowed us to detect modified forms of GAPDH caused by MetAP2 inhibition. Importantly, the concentration response curve for MetAP2 inhibition, as measured by GAPDH processing, correlated well with that of proliferation inhibition. These data supply significant support to the proposal that inhibition of methionine processing by MetAP2 blocks tumor cell growth *in vitro*.

In addition to the *in vitro* work, our GAPDH isoform detection techniques also allowed us to examine MetAP2 inhibition *in vivo*. This was initially accomplished using blood leukocytes isolated from mice dosed with MetAP2 inhibitors. Time-course studies

indicated that it took several days to maximally effect GAPDH isoforms in white cells. Clearly, this time course depends on the half-life of GAPDH in these cells and implies a relatively slow turnover of the protein. The inhibitory effect in mouse blood white cells was also dose-dependent using a number of MetAP2 inhibitors from three distinct chemical classes. Thus, these data indicate that the GAPDH processing seen in cell culture is also seen *in vivo*. The GAPDH isoform measurements were extended to tumors grown in mice and rats (data not shown). Two major observations were made in these studies. First, the inhibitory dose–response curves were similar in tumor tissues compared with WBCs. More importantly, the degree of MetAP2 inhibition as assessed by measuring GAPDH isoform formation correlated well with tumor inhibition using multiple inhibitors. Thus, we were able to establish the *in vivo* correlate to the cellular proliferation studies. These data taken collectively give strong support to the proposal that the antiproliferative/antitumor growth activity seen with these agents is driven by MetAP2 inhibition.

GAPDH as a biomarker for MetAP2 inhibitors has several advantages. It is an abundant cellular protein so it can be easily detected in circulating mononuclear cells and in tumor samples. The N-terminal status of GAPDH reflects the MetAP2 enzyme activity over a period, thus truly representing the consequence of MetAP2 inhibition and better correlating with efficacy of the testing agent. In addition, the GAPDH readout is on MetAP2-specific substrate but not MetAP2 itself, so it can be used for all types of MetAP2 inhibitors. The previously described assays by titrating cellular-free MetAP2 with covalent inhibitors (6, 18) have significant shortcomings compared with the GAPDH biomarker assay. The GAPDH assay format described here may be significantly improved with the advancement of protein mass spectrometry techniques. It could be envisioned that such MS-based assays for GAPDH variants may be developed to analyze clinical samples.

In conclusion, we have shown that the anthranilic acid sulfonamides are potent and selective inhibitors of MetAP2. These compounds show significant activity in mouse tumor growth models and could provide therapeutic benefit in human disease. Additionally, we have developed a biomarker to follow MetAP2 inhibition in tumors and in circulating leukocytes, which has allowed us to demonstrate the *in vivo* correlation of MetAP2 inhibition and tumor suppression in mouse models. This MetAP2 agent and a biomarker should aid in the clinic development of MetAP2 inhibitors for cancer therapy.

Methods

Reagents and Assays. Anthranilic acid sulfonamides including A-800141 were synthesized in the laboratory (20–22). Recombinant human MetAP1 and MetAP2 and activity assays were described as previously (28) and in *SI Text*.

Detection of *GAPDH* N-Terminal Variants. Cells were grown in DMEM media supplemented with 10% FBS in a 37°C incubator with 5% CO_2. WBCs from terminal blood of mice were isolated using a procedure described in *SI Text*. These cell samples were analyzed by IEF followed by Western blot with the monoclonal mouse anti-rabbit GAPDH (RDI-TRK5G4-6C5).

***In Vivo* Studies.** All mice used in these studies were purchased from Charles River Laboratories. All animal studies were conducted within the guidelines established by the internal Institutional Animal Care and Use Committee of Abbott Laboratories. Mouse cornea angiogenesis was carried out as described (10) and in *SI Text*.

ACKNOWLEDGMENTS. We thank Dr. Chang Park for providing the crystallography structure graph used in Fig. 1, Pingping Lou for cell culture work and GAPDH N-terminal sequencing studies, Laura McKay for dosing A-357300 for *in vivo* GAPDH biomarker studies, Dr. John Maris (University of Pennsylvania, Philadelphia) for providing the CHP-134 neuroblastoma cell line, and Drs. Jack Henkin and Scott Warder for helpful discussions and critical comments on the manuscript.

1. Bradshaw RA, Brickey WW, Walker KW (1998) N-terminal processing: the methionine aminopeptidase and N alpha-acetyl transferase families. *Trends Biochem Sci* 23:263–267.
2. Lowther WT, Matthews BW (2000) Structure and function of the methionine aminopeptidases. *Biochim Biophys Acta* 1477:157–167.
3. Arfin SM, *et al.* (1995) Eukaryotic methionyl aminopeptidases: two classes of cobalt-dependent enzymes. *Proc Natl Acad Sci USA* 92:7714–7718.
4. Leszczyniecka M, *et al.* (2006) MAP1D, a novel methionine aminopeptidase family member is overexpressed in colon cancer. *Oncogene* 25:3471–3478.
5. Li X, Chang YH (1995) Amino-terminal protein processing in Saccharomyces cerevisiae is an essential function that requires two distinct methionine aminopeptidases. *Proc Natl Acad Sci USA* 92:12357–12361.
6. Turk BE, *et al.* (1999) Selective inhibition of amino-terminal methionine processing by TNP-470 and ovalicin in endothelial cells. *Chem Biol* 6:823–833.
7. Wang J, Lou P, Henkin J (2000) Selective inhibition of endothelial cell proliferation by fumagillin is not due to differential expression of methionine aminopeptidases. *J Cell Biochem* 77:465–473.
8. Datta B (2000) MAPs and POEP of the roads from prokaryotic to eukaryotic kingdoms. *Biochimie* 82:95–107.
9. Hu X, Addlagatta A, Lu J, Matthews BW, Liu JO (2006) Elucidation of the function of type 1 human methionine aminopeptidase during cell cycle progression. *Proc Natl Acad Sci USA* 103:18148–18153.
10. Wang J, *et al.* (2003) Tumor suppression by a rationally designed reversible inhibitor of methionine aminopeptidase-2. *Cancer Res* 63:7861–7869.
11. Zhang Y, Griffith EC, Sage J, Jacks T, Liu JO (2000) Cell cycle inhibition by the anti-angiogenic agent TNP-470 is mediated by p53 and p21WAF1/CIP1. *Proc Natl Acad Sci USA* 97:6427–6432.
12. Yeh JR, Mohan R, Crews CM (2000) The antiangiogenic agent TNP-470 requires p53 and p21CIP/WAF for endothelial cell growth arrest. *Proc Natl Acad Sci USA* 97:12782–12787.
13. Yeh JR, *et al.* (2006) Targeted gene disruption of methionine aminopeptidase 2 results in an embryonic gastrulation defect and endothelial cell growth arrest. *Proc Natl Acad Sci USA* 103:10379–10384.
14. Bernier SG, Taghizadeh N, Thompson CD, Westlin WF, Hannig G (2005) Methionine aminopeptidases type I, type II are essential to control cell proliferation. *J Cell Biochem* 95:1191–1203.
15. Datta B, Datta R (1999) Induction of apoptosis due to lowering the level of eukaryotic initiation factor 2-associated protein, p67, from mammalian cells by antisense approach. *Exp Cell Res* 246:376–383.
16. Ingber D, *et al.* (1990) Synthetic analogues of fumagillin that inhibit angiogenesis and suppress tumour growth. *Nature* 348:555–557.
17. Kusaka M, *et al.* (1991) Potent anti-angiogenic action of AGM-1470: comparison to the fumagillin parent. *Biochem Biophys Res Commun* 174:1070–1076.
18. Cooper AC, *et al.* (2006) A novel methionine aminopeptidase-2 inhibitor, PPI-2458, inhibits non-Hodgkin's lymphoma cell proliferation *in vitro* and *in vivo*. *Clin Cancer Res* 12:2583–2590.
19. Morowitz MJ, *et al.* (2005) Methionine aminopeptidase 2 inhibition is an effective treatment strategy for neuroblastoma in preclinical models. *Clin Cancer Res* 11:2680–2685.
20. Kawai M, *et al.* (2006) Development of sulfonamide compounds as potent methionine aminopeptidase type II inhibitors with antiproliferative properties. *Bioorg Med Chem Lett* 16:3574–3577.
21. Sheppard GS, *et al.* (2006) Discovery and optimization of anthranilic Acid sulfonamides as inhibitors of methionine aminopeptidase-2: a structural basis for the reduction of albumin binding. *J Med Chem* 49:3832–3849.
22. Wang GT, *et al.* (2007) Lead optimization of methionine aminopeptidase-2 (MetAP2) inhibitors containing sulfonamides of 5,6-disubstituted anthranilic acids. *Bioorg Med Chem Lett* 17:2817–2822.
23. Liu S, Widom J, Kemp CW, Crews CM, Clardy J (1998) Structure of human methionine aminopeptidase-2 complexed with fumagillin. *Science* 282:1324–1327.
24. Griffith EC, *et al.* (1998) Molecular recognition of angiogenesis inhibitors fumagillin and ovalicin by methionine aminopeptidase 2. *Proc Natl Acad Sci USA* 95:15183–15188.
25. Tucker L, *et al.* (2008) Ectopic Expression of Methionine Aminopeptidase-2 Causes Cell Transformation and Stimulates Proliferation. *Oncogene*, in press.
26. Oltersdorf T, *et al.* (2005) An inhibitor of Bcl-2 family proteins induces regression of solid tumours. *Nature* 435:677–681.
27. Kanno T, *et al.* (2002) High expression of methionine aminopeptidase type 2 in germinal center B cells and their neoplastic counterparts. *Lab Invest* 82:893–901.
28. Wang J, *et al.* (2003) Physiologically relevant metal cofactor for methionine aminopeptidase-2 is manganese. *Biochemistry* 42:5035–5042.